Article

pubs.acs.org/Biomac

Design of Functionalized Cellulosic Honeycomb Films: Site-Specific Biomolecule Modification via "Click Chemistry"

William Z. Xu, Xinyue Zhang, and John F. Kadla*

Advanced Biomaterials Chemistry Laboratory, University of British Columbia, Vancouver, British Columbia, Canada V6T 1Z4

Supporting Information

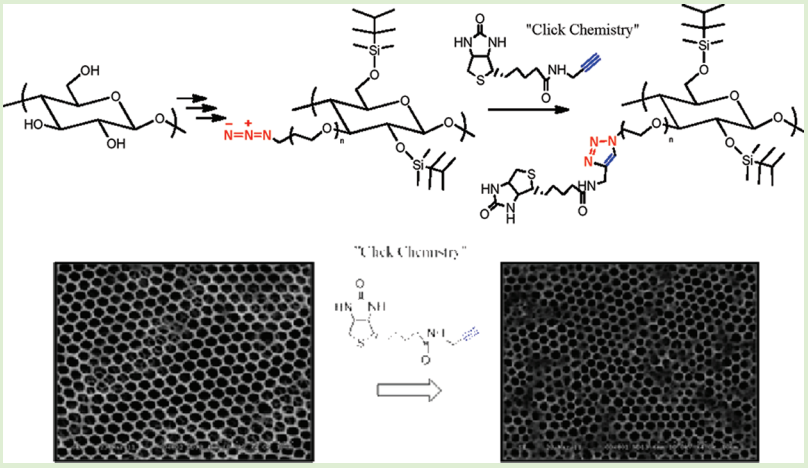

ABSTRACT: Value-added materials from naturally abundant polymers such as cellulose are of significant importance. In particular, cellulosic open-framework structures with controlled chemical functionality of the internal surface have great potential in many biosensor applications. Although various cellulose derivatives can form porous honeycomb structured materials, solubility issues and problems with film formation exist. To address this, we have generated robust cellulosic open-framework structures that can be post-functionalized through site-specific modification. Regioselectively modified amphiphilic cellulose azides, 3-*O*-azidopropoxypoly(ethylene glycol)-2,6-di-*O*-thexyldimethylsilyl cellulosics, were synthesized, and honeycomb-patterned films were readily produced by the simple breath figures method. Changing the degree of polymerization (DP) of the pendent ethylene glycol (EG_{DP}) groups from 22 to 4 increased the corresponding honeycomb film pore diameters from ~1.2 to ~2.6 μm, enabling the potential tuning of pore size. Moreover, these novel azido-functionalized honeycomb films were easily functionalized using Cu(I)-catalyzed alkyne−azide [2 + 3] cycloaddition reaction; biotin was "clicked" onto the azide functionalized cellulosic honeycomb films without any effect to the film structure. These results indicate this system may serve as a platform for the design and development of biosensors.

INTRODUCTION

Bioactive paper is a relatively new field receiving increasing global interest.[1] With increasing concerns over food and water safety, the spread of disease, and the threat of bioterrorism impacting all human life, there is great need for the development of inexpensive bioactive packaging, assays, and sensors.[2] Cellulose, the most abundant biopolymer on earth, is biocompatible and has long been an ideal support material for bioactive systems. Cellulose and its derivatives have served as support matrixes for numerous biomolecules which can be entrapped or encapsulated within the cellulosic matrix or chemically/biochemically coupled.[3−7] Cellulose-based materials offer great potential for the development of pathogen detecting biosensors.

Porous materials with tailored pore sizes and shapes are of growing technological and scientific interest; particularly the development of open-framework structures with controlled chemical functionality of the internal surface or pore lining.[8,9] Such materials offer considerable internal surface area, often highly reactive and ideal for molecular recognition applications such as shape selective catalysis, molecular sieving, selective adsorption/separation, and chemical/biological sensing.[10−15]

Micropatterned or honeycomb pore structures can be formed by various methods including lithography, colloidal crystal templating, emulsion droplet templating, and biotemplating.[16−19] However, these methods are relatively complex and expensive. One of the simplest and most robust methods is the so-called "breath figures" method.[20,21] In this method a thin layer of polymer solution is placed under a humid air stream, which leads to microsized water droplets condensing onto the

Received: September 30, 2011
Revised: November 28, 2011
Published: December 8, 2011

 © 2011 American Chemical Society

cooling surface of the polymer solution. Due to capillary forces, the water droplets rearrange into an ordered hexagonal template, where the polymer precipitates, encapsulating the water droplets and preventing their coalescence.[22] Numerous synthetic polymers, including star, linear, and block copolymers,[22−26] as well as polymer−particle systems[27,28] and semisynthetic biopolymers,[29,30] have been used to form well-structured porous materials using this technique.

Recently, we showed that micropatterned honeycomb films with ordered pore structures of ∼2 μm diameter could be produced using an amphiphilic regioselective cellulose derivative 3-*O*-poly(ethylene glycol)-2,6-di-*O*-thexyldimethylsilyl cellulose.[30] In this system, the amphiphilicity of the polymer was critical for the self-assembly and formation of uniform micropatterned films;[31] the poly(ethylene glycol) segments preferentially interact with the condensing water droplets to direct the self-assembly and, likely, preferentially allocate around the edges of the honeycomb pores. These unique nanostructured materials may serve as a perfect macromolecular platform for the immobilization of bioactive compounds and, therefore, the development of specific recognition systems (e.g., biodefense, pathogen capture, detection, and destruction).

Site-specific modification of biomolecules is an important and challenging area of research. One of the most widely used techniques is the Cu(I)-catalyzed alkyne−azide [2 + 3] cycloaddition or "click" reaction.[32,33] This azide−alkyne cycloaddition offers good reproducibility and a high degree of specificity and is compatible with water, which makes it potentially appropriate for a variety of in vitro and in vivo applications.[34−37] Thus far the use of Cu(I)-catalyzed cycloaddition to functionalize micropatterned films has been limited but offer great potential to control the properties of surfaces while not impacting the bulk properties of the film.[38] Herein, we demonstrate site-specific functionalization of cellulosic micropatterned films using Cu(I)-catalyzed cycloaddition reactions. Biotin, selected as a model bioactive compound, was functionalized with an alkyne linker and "clicked" onto the 3-*O*-azidopropoxypoly(ethylene glycol)-2,6-di-*O*-thexyldimethylsilyl cellulosic micropatterned film.

EXPERIMENTAL SECTION

Materials. Poly(ethylene glycol) MW = 200 (EG_4), poly(ethylene glycol) MW = 600 (EG_{13}), poly(ethylene glycol) MW = 1000 (EG_{22}), dimethylthexylsilyl chloride (TDMSCl, 95%), imidazole, anhydrous *N*,*N*-dimethylacetamide (DMA), anhydrous *N*,*N*-dimethylformamide (DMF), anhydrous dimethyl sulfoxide (DMSO), *p*-toluenesulfonyl chloride (tosyl chloride), sodium azide (NaN_3), sodium azide-1-^{15}N ($Na^{15}N_3$), sodium hydride (60% dispersion in mineral oil), sodium thiosulfate (pentahydrate), triphenylphosphine (PPh_3), 9-borabicyclo-(3.3.1)nonane (9-BBN, 0.5 M in THF), hydrogen peroxide (35%), carbon tetrachloride, (+)-biotin *N*-hydroxysuccinimide (biotin-NHS, ≥98%), propargylamine (98%), triethylamine (≥99%), and tetra-*n*-butylammonium iodide (TBAI) were purchased from Sigma-Aldrich and used as received. Potassium hydroxide, sodium hydroxide, anhydrous magnesium sulfate, potassium iodide, toluene (HPLC grade), chloroform (ACS certified), sodium chloride (ACS certified), sodium bicarbonate (ACS certified), L(+)-ascorbic acid, and cupric sulfate pentahydrate (ACS certified) were purchased from Fisher Scientific and used as received. Tetrahydrofuran (THF, Fisher Scientific), acetone (ACS certified, Fisher Scientific), cellulose (Fluka, Avicel PH-101, ∼50 μm particle size), and anhydrous lithium chloride (Sigma-Aldrich) were dried prior to use.

Characterization. ^1H and ^{13}C NMR spectra were measured using a Bruker AVANCE-300 spectrometer at 25 °C (small molecules) or 40 °C (polymers). Chemical shifts were referenced to tetramethyl silane (TMS; 0.0 ppm). 2D HMQC $^1H/^{15}N$ correlation NMR spectrum was measured using a Bruker AVANCE-600 spectrometer at room temperature. Chemical shifts were referenced to tetramethyl silane (TMS; 0.0 ppm) for ^1H and nitromethane (CH_3NO_2; 0.0 ppm) for ^{15}N. Infrared spectra were obtained with a Perkin-Elmer Spectrum One FT-IR spectrometer (ATR was employed for insoluble samples). Spectra were recorded at a resolution of 4 cm^{-1} and a total of 32 scans. Elemental analysis was measured using a Perkin-Elmer Series II CHNS/O analyzer. Polymer molecular weight was determined by GPC (Agilent 1100) equipped with RI and multiangular light scattering (Wyatt - DAWN HELEOS II) detectors and calibrated with polystyrene standards (columns, Stryagel HR-4 and HR-1; temperature, 35 °C; eluting solvent, THF; flow rate, 0.5 mL/min; sample concentration, 1.6 mg/mL; injection volume, 100 μL). The surface morphology of the cast films was observed with a Hitachi S-2600N scanning electron microscope (SEM).

Allyloxypoly(ethylene glycol) (1a−c). Allyloxypoly(ethylene glycol) (**1a−c**) was synthesized from poly(ethylene glycol) MW = 200 (EG_4), poly(ethylene glycol) MW = 600 (EG_{13}), and poly-(ethylene glycol) MW = 1000 (EG_{22}). Sodium hydride (0.15 mol, 1.5 equiv) was first washed three times (3 × 100 mL) with freshly distilled anhydrous THF. Poly(ethylene glycol) (EG_4; EG_{13}; EG_{22}; 0.15 mol, 1.5 equiv) was then added slowly and stirred in 10 mL of anhydrous THF in an ice bath for 1 h, followed by dropwise addition of allyl bromide (0.1 mol, 1 equiv). The reaction took place at room temperature for 2 days and then at 50 °C for 2 days. After the reaction mixture had cooled to room temperature, 10 mL of distilled water was added, followed by removal of solvent through rotary evaporation. A total of 100 mL of distilled water was then added, followed by extraction with 3 × 70 mL of chloroform. The combined organic phases were washed with 100 mL of 0.1 M $Na_2S_2O_3$ solution, 5 × 100 mL distilled H_2O, 100 mL saturated $NaHCO_3$ solution, and finally 100 mL saturated NaCl solution. The organic phase was subsequently dried over anhydrous $MgSO_4$ and the solvent was removed by rotary evaporation. Yield: **1a** (from EG_4) 72%; **1b** (from EG_{13}) 67%; **1c** (from EG_{22}) 66%. ^1H NMR ($CDCl_3$, 300 MHz) δ (ppm): 2.88 (s, 1H), 3.42−3.78 (m, 16.5/52.9/89.3H), 3.94 (d, J = 5.26 Hz, 2H), 5.09 (d, J = 10.08 Hz, 1H), 5.19 (d, J = 17.10 Hz, 1H), 5.77−5.90 (m, 1H). ^{13}C NMR ($CDCl_3$, 75.4 MHz) δ (ppm): 61.4 (O−CH_2-$\underline{C}H_2$-OH), 69.2 ($\underline{C}H_2$-O-CH_2-CH=CH_2), 70.1, 70.3, 71.9 (O-$\underline{C}H_2$-CH=CH_2), 72.3 (O-$\underline{C}H_2$-CH_2-OH), 116.8 (O-CH_2-CH=$\underline{C}H_2$), 134.5 (O-CH_2-$\underline{C}H$=CH_2).

Allyloxypoly(ethylene glycol) Tosylate (2a−c). Allyloxypoly-(ethylene glycol) tosylate (**2a−c**) was synthesized from allyloxypoly-(ethylene glycol) (**1a−c**). Allyloxypoly(ethylene glycol) (0.066 mol) was dissolved in 10/40 mL distilled H_2O/THF. KOH (0.092 mol, 1.4 equiv) was added and the solution was cooled in an ice bath. A tosyl chloride (0.073 mol, 1.1 equiv) solution in 50 mL of THF was added dropwise and reacted at 0−5 °C for 4 h and then at room temperature for 18 h. The solvent was then removed by rotary evaporation, and 100 mL of distilled H_2O was added, followed by extraction with 3 × 70 mL chloroform. The combined organic phases were washed with 2 × 100 mL distilled H_2O, 100 mL of 0.1 N HCl, 100 mL of saturated $NaHCO_3$ solution, and 100 mL of saturated NaCl solution. The organic phase was subsequently dried over anhydrous $MgSO_4$ and the solvent (chloroform) was removed by rotary evaporation. Yield: **2a** 85%; **2b** 86%; **2c** 86%. ^1H NMR ($CDCl_3$, 300 MHz) δ (ppm): 2.38 (s, 3H), 3.43−3.70 (m, 14.5/50.9/87.3H), 3.96 (d, J = 5.26 Hz, 2H), 4.09 (t, J = 4.82 Hz, 2H), 5.11 (d, J = 10.08 Hz, 1H), 5.21 (d, J = 17.10 Hz, 1H), 5.78−5.91 (m, 1H), 7.28 (d, J = 8.33 Hz, 2H), 7.73 (d, J = 7.89 Hz, 2H). ^{13}C NMR ($CDCl_3$, 75.4 MHz) δ (ppm): 21.4 (C_6H_4-$\underline{C}H_3$), 68.4 (O−CH_2-$\underline{C}H_2$-O-tosyl), 69.1, 69.2 ($\underline{C}H_2$-O-CH_2-CH=CH_2), 70.4, 70.5 (O-$\underline{C}H_2$-CH_2-O-tosyl), 72.0 (O-$\underline{C}H_2$-CH=CH_2), 116.8 (O-CH_2-CH=$\underline{C}H_2$), 127.7 ($\underline{C}_6H_4$-CH_3), 129.6 ($\underline{C}_6H_4$-CH_3), 132.8 ($\underline{C}_6H_4$-CH_3), 134.6 (O-CH_2-$\underline{C}H$=CH_2), 144.6 ($\underline{C}_6H_4$-CH_3).

Allyloxypoly(ethylene glycol) Iodide (3a−c). Allyloxypoly-(ethylene glycol) iodide (**3a−c**) was synthesized from allyloxypoly-(ethylene glycol) tosylate (**2a−c**). Allyloxypoly(ethylene glycol)

Scheme 1. Synthetic Scheme for the Preparation of 3-N_3EG-2,6-TDMS Cellulose[a]

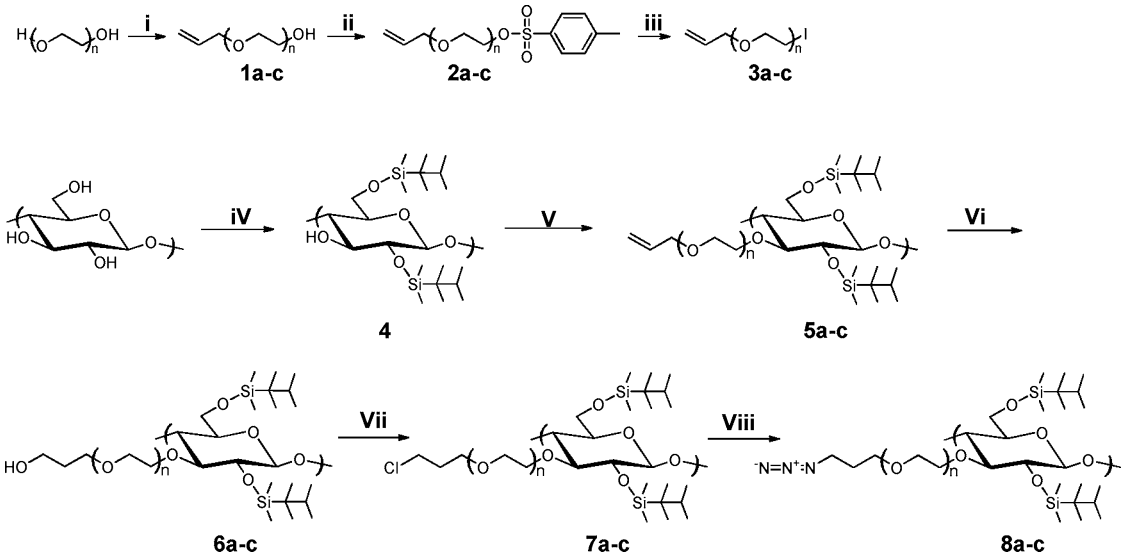

[a]Note: n = 4 for **a**, n = 13 for **b**, and n = 22 for **c**. Reagents and conditions: (i) allyl bromide, NaH, THF; (ii) tosyl chloride, KOH, H_2O/THF; (iii) KI, acetone; (iv) TDMSCl, imidazole, DMA, LiCl; (v) **3a**–**c**, NaH, TBAI, THF; (vi) 9-BBN, NaOH, H_2O_2, THF; (vii) PPh_3, CCl_4, DMA; (viii) NaN_3, THF, DMA.

tosylate (0.056 mol) was dissolved in 224 mL of dry acetone, followed by addition of potassium iodide (0.224 mol, 4 equiv). The mixture was refluxed for 18 h and then cooled to room temperature. The solvent was removed by rotary evaporation and 100 mL of distilled H_2O was then added, followed by extraction with 3 × 70 mL chloroform. The combined organic phases were washed with 100 mL of 0.1 M $Na_2S_2O_3$ solution, 3 × 100 mL of distilled H_2O, 100 mL of saturated $NaHCO_3$ solution, and 100 mL of saturated NaCl solution. The organic phase was subsequently dried over anhydrous $MgSO_4$ and the solvent was removed by rotary evaporation. Yield: **3a** 95%; **3b** 95%; **3c** 82%. ^{1}H NMR ($CDCl_3$, 300 MHz) δ (ppm): 3.19 (t, J = 6.80 Hz, 2H), 3.47–3.64 (m, 12.5/48.9/85.3H), 3.69 (t, J = 7.02 Hz, 2H), 3.95 (d, J = 5.26 Hz, 2H), 5.10 (d, J = 10.52 Hz, 1H), 5.20 (d, J = 17.10 Hz, 1H), 5.78–5.91 (m, 1H). ^{13}C NMR ($CDCl_3$, 75.4 MHz) δ (ppm): 2.8 (O-CH_2-CH_2-I), 69.2 (CH_2-O-CH_2-CH=CH_2), 70.0 (O-CH_2-CH_2-I), 70.3, 71.7, 71.9 (O-CH_2-CH=CH_2), 116.7 (O-CH_2-CH=CH_2), 134.5 (O-CH_2-CH=CH_2).

2,6-Di-*O*-thexyldimethylsilyl Cellulose (2,6-TDMS Cellulose; 4). 2,6-Di-*O*-thexyldimethylsilyl cellulose (2,6-TDMS cellulose; **4**) was synthesized according to the procedure of Koschella et al.[39] with a slight modification.[30,40] Cellulose (2.0 g, 0.012 mol) was suspended in 100 mL of DMA and stirred at 120 °C for 2 h. The slurry was then cooled to 100 °C, and lithium chloride (6.0 g, 0.14 mol) was added and allowed to stir for 30 min. The mixture was then cooled to room temperature and stirred overnight to afford a clear viscous solution. Imidazole (4.0 g, 0.060 mol) was added to the solution and stirred for 1 h, followed by dropwise addition of TDMSCl (12.5 mL, 0.060 mol). The solution was stirred for an additional 1 h before being heated to 70 °C and stirred for 4 h. The reaction mixture was then heated to 100 °C and stirred for 24 h. After that, the reaction mixture was cooled to room temperature and poured slowly into 150 mL of pH 7 buffer solution. The crude product was subsequently isolated by filtration and washed with H_2O, ethanol, and methanol, respectively. Dissolving the crude product in chloroform and precipitating in methanol afforded the purified product as a white powder. Yield: 4.9 g, 89%. Elemental analysis: DS 1.92; calculated for DS = 2: C, 59.14%; H, 10.38%. Found: C, 58.92%; H, 10.32%. FTIR (cm^{-1}): 3508 (ν_{OH}), 2957 ($\nu_{CH_3(as)}$), 2871 ($\nu_{CH_3(s)}$), 1465 ($\delta_{CH_3,CH2(as)}$), 1378 ($\delta_{CH_3(s)}$), 1252 (δ_{Si-C}), 1118 (ν_{Si-O-C}), 1078, 1037 ($\nu_{C-O-C(AGU)}$), 835, 778 ($\nu_{Si-C/Si-O-C}$). ^{13}C NMR (C_6D_6, 313 K, 75.4 MHz) δ (ppm): −3.5–34.8 (TDMS group), 60.9 (C6), 73.1–77.4 (C5∼C2), 102.8 (C1).

3-*O*-Allyloxypoly(ethylene glycol)-2,6-di-*O*-thexyldimethylsilyl Cellulose (3-AllyloxyEG-2,6-TDMS Cellulose; 5a–c). 3-*O*-Allyloxypoly(ethylene glycol)-2,6-di-*O*-thexyldimethylsilyl cellulose (3-allyloxyEG-2,6-TDMS cellulose; **5a**–**c**) was synthesized from 2,6-TDMS cellulose (**4**) and allyloxypoly(ethylene glycol) iodide (**3a**–**c**). Sodium hydride (45 mmol, 10 equiv) was first washed three times (3 × 40 mL) with freshly distilled anhydrous THF, and then 2,6-TDMS cellulose (2.0 g, 4.5 mmol) and TBAI (0.45 mmol, 0.1 equiv) were added and stirred in 40 mL of anhydrous THF in an ice bath for 1 h, followed by dropwise addition of **3a**–**c** (45 mmol, 10 equiv). The reaction took place at room temperature for 5 days. It was then quenched with 40 mL of methanol. The reaction mixture was precipitated into 300 mL of pH 7 buffer solution. The crude product was subsequently isolated by filtration and washed with H_2O, ethanol, and methanol, respectively. Further purification was done by dissolving the crude product in chloroform and precipitating in methanol to afford a white powder. Purified product: DS by ^{1}H NMR: **5a**, 0.47; **5b**, 0.37; **5c**, 0.45. Yield: **5a**, 2.01 g, 81%; **5b**, 1.62 g, 53%; **5c**, 1.75 g, 43%. FTIR (cm^{-1}): 3508 (ν_{OH}), 2957 ($\nu_{CH3(as)}$), 2869 ($\nu_{CH3(s)}$), 1648 ($\nu_{C=C}$), 1465 ($\delta_{CH3,CH2(as)}$), 1377 ($\delta_{CH3(s)}$), 1252 (δ_{Si-C}), 1118 (ν_{Si-O-C}, $_{C-O-C(EG)}$), 1080, 1037 ($\nu_{C-O-C(AGU)}$), 834, 778 ($\nu_{Si-C/Si-O-C}$). ^{1}H NMR ($CDCl_3$, 300 MHz) δ (ppm): 0.13–1.65 (TDMS group), 3.31–4.38 (AGU), 3.65 (EG), 4.03 (d, 2H) 5.18 (d, J = 9.21 Hz, 1H), 5.28 (d, J = 17.10 Hz, 1H), 5.86–5.99 (m, 1H). ^{13}C NMR ($CDCl_3$, 75.4 MHz) δ (ppm): −3.5–34.3 (TDMS group), 69.6, 70.7 (EG), 72.2 (CH_2-CH=CH_2, 116.9 (CH_2-CH=CH_2), 134.9 (CH_2-CH=CH_2).

3-*O*-Hydroxypropoxypoly(ethylene glycol)-2,6-di-*O*-thexyldimethylsilyl Cellulose (3-HOEG-2,6-TDMS Cellulose; 6a–c). 3-*O*-Hydroxypropoxypoly(ethylene glycol)-2,6-di-*O*-thexyldimethylsilyl cellulose (3-HOEG-2,6-TDMS cellulose; **6a**–**c**) was synthesized from **5a**–**c**. Compounds **5a**–**c** (0.75 mmol allyloxy group; **5a**, 880 mg; **5b**, 1.37 g; or **5c**, 1.50 g) were dissolved in 36 mL of freshly distilled anhydrous THF, followed by the addition of 18 mL of 0.5 M 9-BBN (12 equiv) in THF. The mixture was stirred at 75 °C for 3 h and subsequently cooled down to 0–5 °C with an ice bath. Distilled water was then added dropwise to eliminate unreacted 9-BBN (until no bubbling was observed). Subsequently, 18 mL of 3 M NaOH solution and 15.6 mL of 35% H_2O_2 were added dropwise, respectively. The reaction mixture was further stirred at room temperature for 16 h. THF was then removed by rotary evaporation and 90 mL of distilled H_2O was added. The crude product was filtered off and washed with distilled water and methanol, respectively. Further

dx.doi.org/10.1021/bm201364r | Biomacromolecules 2012, 13, 350–357

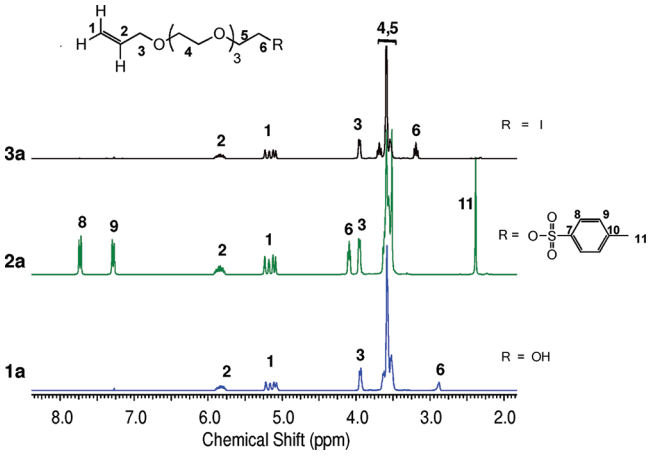

Figure 1. ^{1}H NMR spectra of the synthesized poly(ethylene glycol) derivatives **1a**, **2a**, and **3a**.

purification of the product was carried out by dissolving crude product in chloroform and precipitating in methanol. Yield: **6a**, 687 mg, 77%; **6b**, 1.08 g, 78%; **6c**, 1.30 g, 86%. FTIR (cm^{-1}): 3510 (ν_{OH}), 2957 ($\nu_{CH_3(as)}$), 2870 ($\nu_{CH_3(s)}$), 1465 ($\delta_{CH_3,CH_2(as)}$), 1378 ($\delta_{CH_3(s)}$), 1252 (δ_{Si-C}), 1118 ($\nu_{Si-O-C,C-O-C(EG)}$), 1080, 1037 ($\nu_{C-O-C(AGU)}$), 834, 778 ($\nu_{Si-C/Si-O-C}$). ^{1}H NMR ($CDCl_3$, 300 MHz) δ (ppm): 0.07−1.65 (TDMS group), 1.83 (q, J = 5.48 Hz, 2H, -O-CH_2-C$\underline{H}_2$-CH_2-OH), 3.32−4.37 (AGU), 3.65 (EG). ^{13}C NMR ($CDCl_3$, 75.4 MHz) δ (ppm): −3.5−25.2, 34.3 (TDMS group), 32.2 (-O-CH_2-$\underline{C}H_2$-CH_2-OH), 60.7 (-O-CH_2-CH_2-$\underline{C}H_2$-OH), 70.4, 70.7 (EG).

3-*O*-Chloropropoxypoly(ethylene glycol)-2,6-di-*O*-thexyldimethylsilyl Cellulose (3-Cl-EG-2,6-TDMS Cellulose; 7a−c). 3-*O*-Chloropropoxypoly(ethylene glycol)-2,6-di-*O*-thexyldimethylsilyl cellulose (3-Cl-EG-2,6-TDMS cellulose; **7a−c**) was synthesized from **6a−c**. Compounds **6a−c** (0.50 mmol hydroxypropoxy group; **6a**, 595 mg; **6b**, 924 mg; or **6c**, 1.02 g) were dissolved in 6 mL of CCl_4, followed by the addition of 24 mL DMA and 524 mg PPh_3 (2 mmol, 4 equiv). The mixture was stirred at 90 °C for 18 h and subsequently cooled to room temperature and precipitated into 150 mL of methanol. The crude product was filtered off and washed with methanol. Further purification was done by dissolving the crude product in chloroform and precipitating in methanol. Yield: **7a**, 518 mg, 86%; **7b**, 678 mg, 73%; **7c**, 956 mg, 93%. FTIR (cm^{-1}): 3502 (ν_{OH}), 2957 ($\nu_{CH_3(as)}$), 2870 ($\nu_{CH_3(s)}$), 1465 ($\delta_{CH_3,CH_2(as)}$), 1378 ($\delta_{CH_3(s)}$), 1252 (δ_{Si-C}), 1118 ($\nu_{Si-O-C,\ C-O-C(EG)}$), 1080, 1037 ($\nu_{C-O-C(AGU)}$), 834, 778 ($\nu_{Si-C/Si-O-C}$). ^{1}H NMR ($CDCl_3$, 300 MHz) δ (ppm): 0.05−1.65 (TDMS group), 2.03 (q, J = 6.14 Hz, 2H, -O-CH_2-C$\underline{H}_2$-CH_2-Cl),

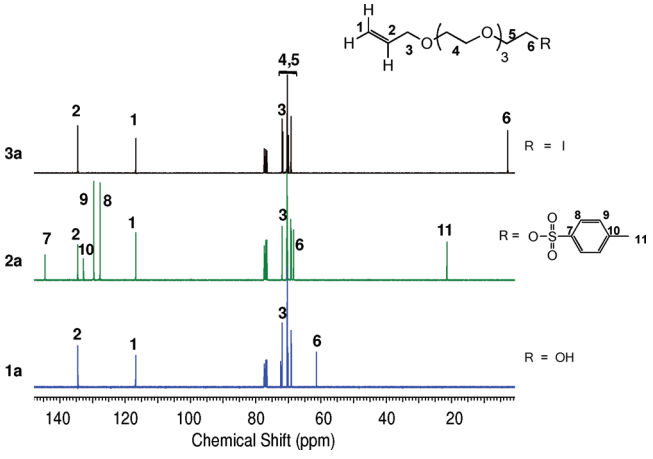

Figure 2. ^{13}C NMR spectra of the synthesized poly(ethylene glycol) derivatives **1a**, **2a**, and **3a**.

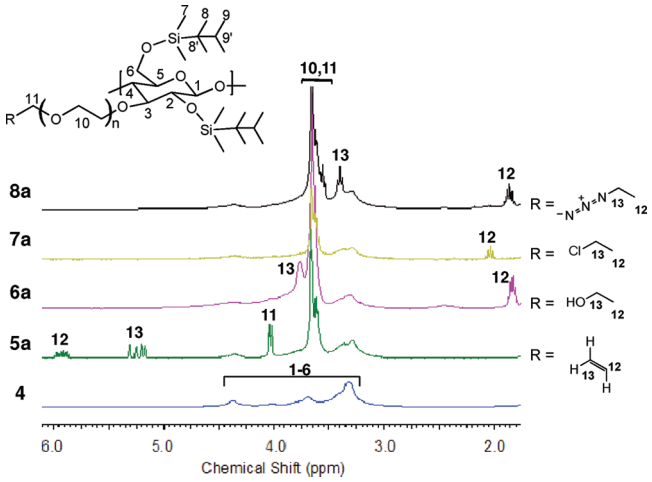

Figure 3. ^{1}H NMR spectra of the synthesized 2,6-TDMS cellulose derivatives **4**, **5a**, **6a**, **7a**, and **8a**.

3.29−4.36 (AGU), 3.66 (EG). ^{13}C NMR ($CDCl_3$, 75.4 MHz) δ (ppm): −3.5−25.2, 34.3 (TDMS group), 32.8 (-O-CH_2-$\underline{C}H_2$-CH_2-Cl), 41.9 (-O-CH_2-CH_2-$\underline{C}H_2$-Cl), 67.7 (-O-$\underline{C}H_2$-CH_2-CH_2-Cl), 70.6 (EG).

3-*O*-Azidopropoxypoly(ethylene glycol)-2,6-di-*O*-thexyldimethylsilyl Cellulose (3-N_3EG-2,6-TDMS Cellulose; 8a−c). 3-*O*-Azidopropoxypoly(ethylene glycol)-2,6-di-*O*-thexyldimethylsilyl cellulose (3-N_3EG-2,6-TDMS cellulose; **8a−c**) was synthesized from **7a−c**. Compounds **7a−c** (0.40 mmol chloro group; **7a**, 482 mg; **7b**, 746 mg; or **7c**, 816 mg) were dissolved in 8 mL of freshly distilled anhydrous THF, followed by the addition of 40 mL of DMA and 520 mg NaN_3 or $Na^{15}N_3$ (8.0 mmol, 20 equiv). The mixture was stirred at 80 °C for 18 h and subsequently cooled to room temperature and precipitated into 160 mL of distilled water. The crude product was filtered off and washed with distilled water and then methanol. Further purification was done by dissolving the crude product in chloroform and precipitating in methanol. Yield: **8a**, 420 mg, 86%; **8b**, 589 mg, 79%; **8c**, 765 mg, 93%. **8a**, M_w = 257 kDa, PDI = 1.70. FTIR (cm^{-1}): 3514 (ν_{OH}), 2957 ($\nu_{CH_3(as)}$), 2869 ($\nu_{CH_3(s)}$), 2098 ($\nu_{N_3(as)}$), 1465 ($\delta_{CH_3,CH_2(as)}$), 1378 ($\delta_{CH_3(s)}$), 1251 (δ_{Si-C}), 1118 ($\nu_{Si-O-C,C-O-C(EG)}$), 1079, 1037 ($\nu_{C-O-C(AGU)}$), 835, 778 ($\nu_{Si-C/Si-O-C}$). ^{1}H NMR ($CDCl_3$, 300 MHz) δ (ppm): 0.05−1.63 (TDMS group), 1.86 (q, J = 6.36 Hz, 2H, -O-CH_2-C$\underline{H}_2$-CH_2-N_3), 3.28−4.36 (AGU), 3.40 (t, J = 6.58 Hz, 2H, -O-CH_2-CH_2-C$\underline{H}_2$-N_3), 3.66 (EG). ^{13}C NMR ($CDCl_3$, 75.4 MHz) δ (ppm): −3.5−25.2, 34.3 (TDMS group), 29.3 (-O-CH_2-$\underline{C}H_2$-CH_2-N_3), 48.6 (-O-CH_2-CH_2-$\underline{C}H_2$-N_3), 67.9 (-O-$\underline{C}H_2$-CH_2-CH_2-N_3), 70.6

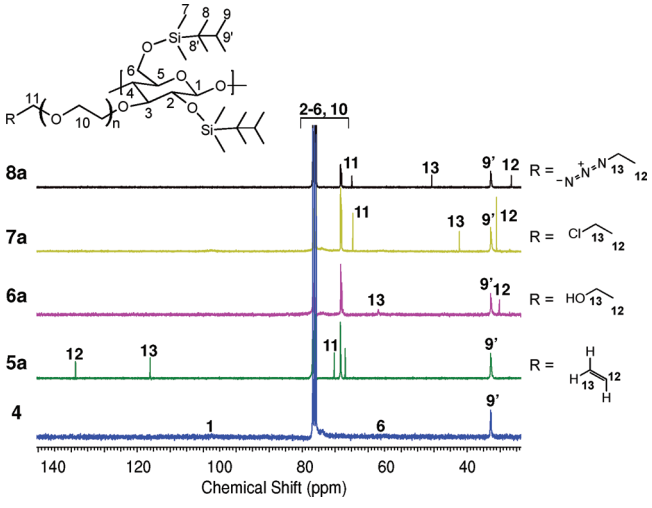

Figure 4. ^{13}C NMR spectra of the synthesized 2,6-TDMS cellulose derivatives **4**, **5a**, **6a**, **7a**, and **8a**.

dx.doi.org/10.1021/bm201364r | *Biomacromolecules* 2012, 13, 350−357

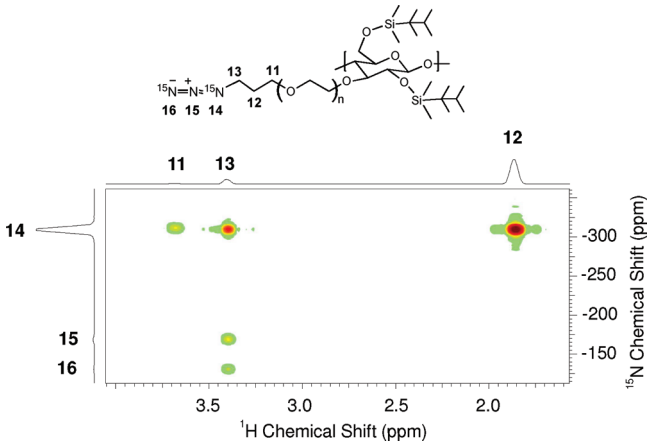

Figure 5. 2D HMQC long-range $^{1}H/^{15}N$ correlation $J_{(NH)}$ = 10 Hz NMR spectrum of **8a** synthesized using ^{15}N-labeled NaN_3.

(EG). ^{15}N NMR ($CDCl_3$, 600 MHz) δ (ppm): −309.4 (-CH_2-N=N$^+$=N$^-$), −169.4 (-CH_2-N=N$^+$=N$^-$), −131.0 (-CH_2-N=N$^+$=N$^-$).

Alkynated Biotin (9). Alkynated biotin (**9**) was synthesized according to the procedure of Lin et al.[41] with a simplified workup procedure. To a solution of biotin-NHS (100 mg, 0.29 mmol) in 6 mL of DMF, 30 μL of propargylamine (26 mg, 0.46 mmol), and 90 μL of triethylamine (60 mg, 0.60 mmol) were added. After stirring at room temperature for 24 h, the reaction mixture was placed under reduced pressure to remove volatile molecules, leaving a dried crude product (114 mg). ^{1}H NMR (DMSO-d_6, 300 MHz) δ (ppm): 1.20−1.70 (6H), 2.08 (t, J = 7.23 Hz, 2H), 2.50 (1H), 2.57 (d, J = 12.28 Hz, 1H), 2.82 (dd, J = 12.28, 4.82 Hz, 1H), 3.07 (2H), 3.83 (2H), 4.13 (1H), 4.30 (1H), 6.34 (1H), 6.41 (1H), 8.21 (1H). ^{13}C NMR (DMSO-d_6, 75.4 MHz) δ (ppm): 25.1, 27.7, 28.0, 28.2, 34.8, 39.8, 55.4, 59.4, 61.0, 72.8, 81.3, 162.7, and 171.8.

3-*O*-Biotinpoly(ethylene glycol)-2,6-di-*O*-thexyldimethylsilyl Cellulose (3-biotinEG-2,6-TDMS Cellulose; 10a−c). 3-*O*-Biotinpoly(ethylene glycol)-2,6-di-*O*-thexyldimethylsilyl cellulose (3-biotinEG-2,6-TDMS cellulose; **10a−c**) was synthesized by reacting **8a−c** with **9**. To a solution of 42 mg (0.034 mmol azido group) **8a** in 1 mL of THF was added a solution of the above synthesized alkynated biotin (114 mg, ∼0.29 mmol) in 1 mL of DMSO, followed by the addition of 4.3 mg (0.017 mmol) cupric sulfate pentahydrate and 6 mg (0.034 mmol) L(+)-ascorbic acid. After being stirred at 40 °C for 3 days, the reaction mixture was cooled down to room temperature and then precipitated into 20 mL of distilled water and subsequently washed with water and methanol. The product was dried in vacuo. Yield: 39.4 mg.

Preparation of Honeycomb Films of 3-*O*-Azidopropoxypoly(ethylene glycol)-2,6-di-*O*-thexyldimethylsilyl Cellulose. Micropatterned films were prepared by applying 10 μL of neat solution (1% **8a−c** in toluene) onto a glass slide in a humid environment (flow rate, 700 mL/min; relative humidity, 70−80%; room temperature).[30]

Formation of Honeycomb Membranes of 3-*O*-Biotinpoly(ethylene glycol)-2,6-di-*O*-thexyldimethylsilyl Cellulose. Linking biotin to the surface of honeycomb membranes of **8a−c** was conducted by immersing the honeycomb membranes in a solution of alkynated biotin **9** (57 mg, ∼0.14 mmol), 4.3 mg (0.017 mmol) cupric sulfate pentahydrate, and 6 mg (0.034 mmol) L(+)-ascorbic acid in 1 mL of DMSO at 45 °C for 3 days, followed by washing with distilled water and methanol, and then drying before characterization with SEM and FTIR. FTIR (cm^{-1}): 2956 ($\nu_{CH_3(as)}$), 2869 ($\nu_{CH_3(s)}$), 1700 ($\nu_{C=O}$), 1464 ($\delta_{CH_3,CH_2(as)}$), 1377 ($\delta_{CH_3(s)}$), 1251 (δ_{Si-C}), 1115 ($\nu_{Si-O-C,C-O-C(EG)}$), 1079, 1036 ($\nu_{C-O-C(AGU)}$), 832, 779 ($\nu_{Si-C/Si-O-C}$).

RESULTS AND DISCUSSION

Recently we demonstrated that open-framework structures with uniform pores of ∼2 μm diameter could be produced from amphiphilic 3-*O*-poly(ethylene glycol) monomethyl ether-2,6-di-*O*-thexyldimethylsilyl cellulose by breadth figures method.[30] Increasing the chain length of the pendent poly(ethylene glycol) monomethyl ether (EGM) groups dramatically improved film formation and pore uniformity. However, the degree of EGM substitution (DS_{EGM}) was very low, ∼0.1−0.2 (theoretical 1.0), likely due to the poor reactivity of the tosylated-EGM reagent. Using the corresponding EGM-iodide improved the DS_{EGM} to ∼0.5 after optimization of reaction conditions (5 equiv EGM-I; 10 equiv NaH; $TBAI_{cat}$; 4 days).[40] Unfortunately, these conditions are not suitable for derivatization using ethylene glycols; condensation of the HO-EG-I occurred, rapidly consuming the reagent and resulting in very low degrees of substitution (DS_{EG} < 0.1). Therefore, a protection scheme to maximize EG substitution as well as enable subsequent conversion to the desired cellulosic azide for the site-specific azide−alkyne cycloaddition was developed and is outlined in Scheme 1.

A key reagent in this multistep synthesis is the allyloxypoly(ethylene glycol) iodide (**3a−c**). It was prepared from poly(ethylene glycol) via a three-step conversion (Scheme 1). Accordingly, poly(ethylene glycol) (EG_4, EG_{13}, and EG_{22}) was first protected by reacting allyl bromide with one of the EG hydroxyl groups to form allyloxypoly(ethylene glycol) **1a−c**. The second hydroxyl group was then converted to the corresponding tosylate **2a−c**, followed by further conversion to the iodide **3a−c**. Although the reaction stoichiometry was selected to allylate only one of the hydroxyl groups, a small amount of poly(ethylene glycol) diallyl ether was formed and some unreacted poly(ethylene glycol) remained after the reaction. The unreacted poly(ethylene glycol) was removed through intensive washing, while the diallyl ether was not removed as it did not affect the subsequent reaction.

Monoallylation of the EG and further conversion to the allyl-EG-I was confirmed by ^{1}H and ^{13}C NMR. Figure 1 shows the ^{1}H NMR spectra for compounds **1a**, **2a**, and **3a**, respectively. The multiplet centered at 5.82 ppm and the doublets at 5.19, 5.09, and 3.94 ppm are assigned to the methyne proton (CH_2=C$\underline{H}$-CH_2) and methylene protons ($C\underline{H}_2$=CH−CH_2 and CH_2=CH-$C\underline{H}_2$) on the allyl group, respectively. The shoulder at 2.88 ppm in the spectrum of **1a** corresponds to the free hydroxyl group of the allyloxypoly(ethylene glycol). After tosylation (**2a**) the spectrum is significantly changed; new peaks appear at 7.73, 7.28, and 2.38 ppm, attributed to the aromatic ring ($C_6\underline{H}_4$-) and methyl (C_6H_4-$C\underline{H}_3$) protons of the tosyl group, the broad hydroxyl peak at 2.88 ppm has disappeared, and the triplet associated with the methylene protons adjacent to the formerly free hydroxyl group (O-CH_2-$C\underline{H}_2$-OH) has shifted downfield to 4.09 ppm. Finally, the spectrum of the allyloxypoly(ethylene glycol) iodide **3a** is marked by two new triplets at 3.70 (O-$C\underline{H}_2$-CH_2-I) and 3.19 ppm (O-CH_2-$C\underline{H}_2$-I) along with the disappearance of the peaks related to the tosyl group.

Similarly, the ^{13}C NMR spectra (Figure 2) show the peaks associated with the allyl group at 134.5, 116.8, and 71.9 ppm. The tosylated product **2a**, again has the additional ^{13}C peaks associated with the tosyl group at 144.6, 132.8, 129.6, 127.7, and 21.4 ppm, and the peak of the methylene group now next to the tosyl group (O-CH_2-$C\underline{H}_2$-O-tosyl) has shifted from

dx.doi.org/10.1021/bm201364r | Biomacromolecules 2012, 13, 350−357

Scheme 2. Synthetic Scheme for the Preparation of Alkynated Biotin (9) and Reaction with 3-N_3EG-2,6-TDMS Cellulose via Cu-Catalyzed [2 + 3] Cycloaddition Reaction[a]

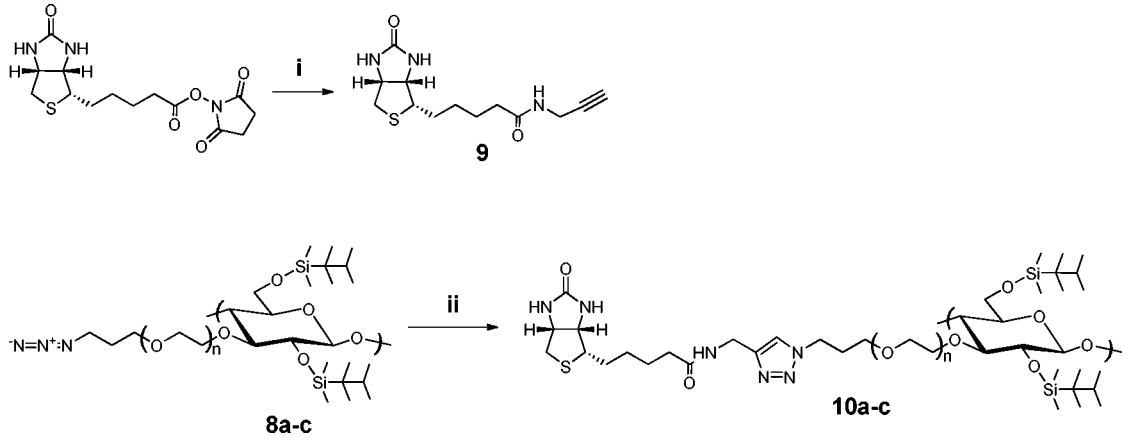

[a]Note: n = 4 for **a**, n = 13 for **b**, and n = 22 for **c**. Reagents and conditions: (i) propargylamine, triethylamine, DMF; (ii) cupric sulfate pentahydrate, L(+)-ascorbic acid, DMSO.

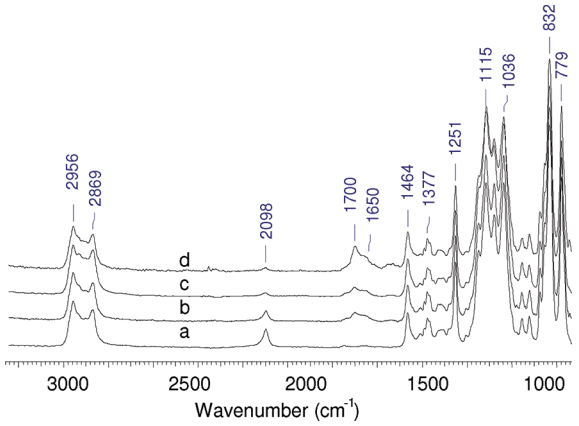

Figure 6. ATR-FTIR spectra for (a) **8a** before and (b) **8a** after the surface "click reaction"; (c) **8c** after the surface "click reaction"; and (d) **10a** (solution "click reaction" using **8a**).

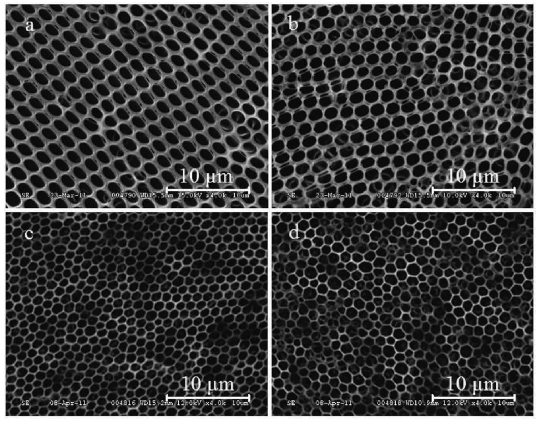

Figure 7. SEM images of honeycomb membranes for **8a** and **8c** before (a and c) and after (b and d) the surface "click reaction", respectively.

61.4 ppm (**1a**) to 68.4 ppm (**2a**). Conversion to the iodinated-allyl-poly(ethylene glycol) **3a** sees complete disappearance of the tosyl related peaks and the methylene peak adjacent to the iodo group (O-CH_2-$\underline{CH_2}$-I) is now shifted far upfield to 2.8 ppm.

As per Scheme 1, the allyloxypoly(ethylene glycol) iodides (**3a−c**) were then reacted with regioselective 2,6-di-*O*-TDMS cellulose (**4**) to produce the 3-allyloxyEG-2,6-TDMS cellulose (**5a−c**). Again, using ^{1}H NMR (Figure 3) and ^{13}C NMR (Figure 4) spectroscopy the introduction of the allyloxyEG group onto the C3-position of the 2,6-di-*O*-TDMS cellulose was readily apparent. The methyne (5.86−5.99 ppm) and methylene (5.28/5.18 and 4.03 ppm) protons associated with the allyloxy group (Figure 3), as well as the corresponding carbon signals at 134.9, 116.9, and 72.2 ppm, respectively (Figure 4), along with those associated with the AGU (anhydroglucopyranose unit) clearly confirm the formation of **5a**. Integrating the ^{1}H NMR spectra determined the degree of substitution to be ∼0.5, according to eq 1:

$$\mathrm{DS} = \frac{7 \int (5.86\text{-}5.99\ \mathrm{ppm})}{\int (2.5\text{-}5.0\ \mathrm{ppm}) - [(4n+2) \int (5.86\text{-}5.99\ \mathrm{ppm})]}$$

A total of 7 is the number of protons associated with the AGU, and n is the degree of polymerization of the poly(ethylene glycol).

The terminal allyloxy group of the pendent EG chain was subsequently oxidized to the corresponding hydroxypropoxy group to afford 3-HOEG-2,6-TDMS cellulose (**6a−c**) in relatively good yields (77−86%). Both the ^{1}H NMR (Figure 3) and ^{13}C NMR (Figure 4) spectra show the disappearance of the olefinic peaks and the concurrent appearance of the new peaks associated with the hydroxypropoxy group; specifically, the methylene groups at 1.83/32.2 ppm (O-CH_2-$\underline{CH_2}$-CH_2-OH) and 3.80/60.7 ppm (O-CH_2-CH_2-$\underline{CH_2}$-OH). Further conversion to 3-ClEG-2,6-TDMS cellulose (**7a−c**) by reaction with PPh_3 and CCl_4 lead to a slight change in the chemical shift of the corresponding methylene protons (Figure 3). However, the ^{13}C NMR (Figure 4) spectrum clearly showed the successful transformation, with the terminal carbon (-O-CH_2-CH_2-$\underline{CH_2}$-Cl) shifting upfield to 41.9 ppm. Finally the desired product 3-N_3EG-2,6-TDMS cellulose (**8a−c**) was readily produced by reacting **7a−c** with NaN_3 in THF/DMA. Conversion of the chloro group (**7a**) to the azido group (**8a**) caused a change in chemical shift of the methylene quintet (O-CH_2-$\underline{CH_2}$-CH_2-N_3) from 2.03 ppm (**7a**) to 1.86 ppm (**8a**) along with a new triplet at 3.40 ppm associated with the methylene protons next

dx.doi.org/10.1021/bm201364r | *Biomacromolecules* 2012, 13, 350−357

to the azido group (O-CH_2-CH_2-$C\underline{H}_2$-N_3). Likewise, the corresponding carbon signals shifted upfield to 29.3 ppm (O-CH_2-$\underline{C}H_2$-CH_2-N_3) and downfield to 48.6 (O-CH_2-CH_2-$\underline{C}H_2$-N_3), respectively.

Further structural conformation of the azido product **8a** (3-*O*-azidopropoxypoly(ethylene glycol)-2,6-di-*O*-thexyldimethylsilyl cellulose) was obtained from 2D HMQC long-range $^1H/^{15}N$ correlation NMR (Figure 5) using the corresponding ^{15}N-labeled derivative. The 2D HMQC NMR clearly shows the azido functionality and the correlation with the three methylene groups (O-CH_2-CH_2-CH_2-$^{15}N{=}N^+{=}{}^{15}N^-$) of the terminal propoxy moiety.

Scheme 2 outlines the synthetic preparation of the alkynated biotin (**9**) and its reaction with 3-N_3EG-2,6-TDMS cellulose via Cu-catalyzed [2 + 3] cycloaddition reaction. To link biotin to the synthesized intermediate **8a**–**c** via "click chemistry", biotin-NHS was reacted with propargylamine to form the corresponding alkynated biotin **9**.[41] As the 3-*O*-azidopropoxypoly(ethylene glycol)-2,6-di-*O*-thexyldimethylsilyl cellulosics (**8a**–**c**) were not soluble in the reaction medium (DMSO), they were first dissolved in a small amount of THF (~42 mg/mL) prior to being introduced into the reaction.

Surprisingly, the products (**10a**–**c**) had very poor solubility in common solvents, including THF, DMSO, DMF, DMA, benzene, toluene, and chloroform. As a result, these materials were not able to be characterized using NMR. However, successful conversion of **8a** to **10a** via "click chemistry" was confirmed by ATR-FTIR (Figure 6a and 6d), with the azido stretching band at 2098 cm^{-1} decreasing significantly while new bands appear at 1700 and 1650 cm^{-1} corresponding to the carbonyl and triazole groups associated with biotin.

The poor solubility of the 3-biotinEG-2,6-TDMS cellulosics (**10a**–**c**) precluded the casting of films. However, the precursor azide molecules (**8a**–**c**) were readily soluble and easily cast to form honeycomb films with uniform pore structures by the breadth figures method. Figure 7 shows the surface morphology of the honeycomb films obtained. Interestingly, increasing the DP of the azidopropoxypoly(ethylene glycol) side chain from 4 (EG_4) to 22 (EG_{22}) substantially decreased the pore size of the honeycomb film from an average diameter of 2.61 (±0.21) μm to 1.2 (±0.29) μm (Figure 7a and c). This observation appears to contradict our previous finding where low DP EG did not form uniform honeycomb films.[30] This apparent discrepancy is likely due to the DS of the EG chains along the TDMS cellulose backbone. In our prior work, the DS of the EG was ~0.1, whereas the materials report here have a DS of ~0.5. As it is known that amphiphilicity dramatically affects honeycomb film formation, it is likely the combination of higher DS with the lower DP EG enabled uniform honeycomb films to be obtained. We are currently investigating the effect of the EG side chain length and the degree of substitution on the formation of these honeycomb membranes.

The 3-N_3EG-2,6-TDMS cellulosic (**8a** and **c**) micropatterned films were then surface functionalized via the Cu-catalyzed [2 + 3] cycloaddition reaction using the alkynated biotin **9**. The reactions were run for 3 days at 45 °C in DMSO. SEM analysis revealed no effect of the site-specific biotinylation on the honeycomb film morphology; Figure 7a vs b and c vs d. Confirmation of the successful surface initiated "click reaction" was made by ATR-FTIR. Again a decrease in the azido band at 2098 cm^{-1} was observed accompanied by the appearance of the carbonyl and triazole bands at 1700 and 1650 cm^{-1} (Figure 6a and c). The spectra obtained for the reactions run using **8a** show a smaller change in the band associated with the azide group (2098 cm^{-1}) compared to that using **8c**; the absorbance changing from 0.21 to 0.12 for **8a** versus 0.11 to 0.03 for **8c**. This implies that significantly more azide groups on films prepared with the longer azidopropoxypoly(ethylene glycol) side chain (N_3EG_{22}) participated in the Cu(I)-catalyzed alkyne–azide [2 + 3] cycloaddition than those with the corresponding N_3EG_4 side chains. This may be due to the longer N_3EG groups being more accessible; they extend further into the reaction medium and, thereby, are more easily modified.

CONCLUSIONS

Regioselectively modified amphiphilic 3-*O*-azidopropoxypoly(ethylene glycol)-2,6-di-*O*-thexyldimethylsilyl cellulosics were synthesized and fully characterized using FTIR and NMR (^1H,^{13}C, $^1H/^{15}N$ HMQC). Biotinylation via Cu(I)-catalyzed alkyne–azide [2 + 3] cycloaddition reaction produced an insoluble product prohibiting honeycomb film formation. However, open-framework cellulosic structures were readily produced from the regioselectively modified amphiphilic cellulose azides using the simple breadth figures method. Changing the DP of the pendent ethylene glycol substituents had a dramatic effect on the pore structure of the resultant honeycomb films; increasing the EG DP from 4 to 22 decreased the average pore diameter from 2.61 (±0.21) to 1.2 (±0.29) μm. Moreover, these novel cellulosic azide honeycomb films could be readily modified via a heterogeneous surface "click reaction". SEM analysis of the films before and after site-specific biotinylation revealed no change in film morphology, while ATR-FTIR analysis indicated the films produced with the longer N_3EG_{22} side chains were more reactive to the cycloaddition. Thus, robust open-framework cellulosic structures capable of site-specific modification can be produced using "click" chemistry, opening the pathway to functional porous materials with controlled chemical functionality.

ASSOCIATED CONTENT

Supporting Information

^1H NMR spectral data for sample **5a**, **5b**, and **5c**, and EG DS calculation data. This material is available free of charge via the Internet at http://pubs.acs.org.

AUTHOR INFORMATION

Corresponding Author

*Phone: (604) 827-5254. Fax: (604) 822-0661. E-mail: john.kadla@ubc.ca.

ACKNOWLEDGMENTS

This work was financially supported by the SENTINEL bioactive paper network. Special thanks go to Ms. Zorana Danilovic, NMR facilities technician at the department of chemistry, UBC, for assistance in the 2D HMQC $^1H/^{15}N$ NMR measurement, and Mr. Derrick Horne, senior EM technician at UBC bioimaging facility, for assistance in the SEM measurements.

REFERENCES

(1) Pelton, R. *Trends Anal. Chem.* **2009**, *28* (8), 925–942.
(2) Martinez, A. W.; Phillips, S. T.; Butte, M. J.; Whitesides, G. M. *Angew. Chem., Int. Ed.* **2007**, *46* (8), 1318–1320.
(3) Tiller, J. C.; Rieseler, R.; Berlin, P.; Klemm, D. *Biomacromolecules* **2002**, *3* (5), 1021–1029.

(4) Turner, M. B.; Spear, S. K.; Holbrey, J. D.; Daly, D. T.; Rogers, R. D. *Biomacromolecules* **2005**, *6* (5), 2497−2502.
(5) Boese, B. J.; Breaker, R. R. *Nucleic Acids Res.* **2007**, *35* (19), 6378−6388.
(6) Pelegrin, M.; Marin, M.; Noel, D.; Del Rio, M.; Saller, R.; Stange, J.; Mitzner, S.; Gunzburg, W. H.; Piechaczyk, M. *Gene Ther.* **1998**, *5* (6), 828−834.
(7) Ali, M. M.; Aguirre, S. D.; Xu, Y. Q.; Filipe, C. D. M.; Pelton, R.; Li, Y. F. *Chem. Commun.* **2009**, *43*, 6640−6642.
(8) Davis, M. E. *Nature* **1993**, *364* (6436), 391−393.
(9) Bradshaw, D.; Claridge, J. B.; Cussen, E. J.; Prior, T. J.; Rosseinsky, M. J. *Acc. Chem. Res.* **2005**, *38* (4), 273−282.
(10) Yanai, N.; Kitayama, K.; Hijikata, Y.; Sato, H.; Matsuda, R.; Kubota, Y.; Takata, M.; Mizuno, M.; Uemura, T.; Kitagawa, S. *Nat. Mater.* **2011**, *10* (10), 787−793.
(11) Risbud, M. V.; Bhonde, R. R. *J. Biomed. Mater. Res.* **2001**, *54* (3), 436−444.
(12) Ma, D.; McHugh, A. J. *J. Membr. Sci.* **2007**, *298* (1−2), 156−168.
(13) Reculusa, S.; Heim, M.; Gao, F.; Mano, N.; Ravaine, S.; Kuhn, A. *Adv. Funct. Mater.* **2011**, *21* (4), 691−698.
(14) Tamada, Y. *Biomacromolecules* **2005**, *6* (6), 3100−3106.
(15) Rossi, A. M.; Wang, L.; Reipa, V.; Murphy, T. E. *Biosens. Bioelectron.* **2007**, *23* (5), 741−745.
(16) Sun, Z. Q.; Li, Y. F.; Wang, Y. F.; Chen, X.; Zhang, J. H.; Zhang, K.; Wang, Z. F.; Bao, C. X.; Zeng, H.; Zhao, B.; Yang, B. *Langmuir* **2007**, *23* (21), 10725−10731.
(17) Gates, B.; Yin, Y. D.; Xia, Y. N. *Chem. Mater.* **1999**, *11* (10), 2827−2836.
(18) Imhof, A.; Pine, D. J. *Nature* **1997**, *389* (6654), 948−951.
(19) Davis, S. A.; Burkett, S. L.; Mendelson, N. H.; Mann, S. *Nature* **1997**, *385* (6615), 420−423.
(20) Francois, B.; Pitois, O.; Francois, J. *Adv. Mater.* **1995**, *7* (12), 1041−1044.
(21) Hoa, M. L. K.; Lu, M.; Zhang, Y. *Adv. Colloid Interface Sci.* **2006**, *121* (1−3), 9−23.
(22) Widawski, G.; Rawiso, M.; Francois, B. *Nature* **1994**, *369* (6479), 387−389.
(23) Stenzel-Rosenbaum, M. H.; Davis, T. P.; Fane, A. G.; Chen, V. *Angew. Chem., Int. Ed.* **2001**, *40* (18), 3428−3432.
(24) Nishikawa, T.; Nishida, J.; Ookura, R.; Nishimura, S. I.; Wada, S.; Karino, T.; Shimomura, M. *Mater. Sci. Eng., C* **1999**, *8*−*9*, 495−500.
(25) Nishikawa, T.; Ookura, R.; Nishida, J.; Arai, K.; Hayashi, J.; Kurono, N.; Sawadaishi, T.; Hara, M.; Shimomura, M. *Langmuir* **2002**, *18* (15), 5734−5740.
(26) Billon, L.; Manguian, M.; Pellerin, V.; Joubert, M.; Eterradossi, O.; Garay, H. *Macromolecules* **2009**, *42* (1), 345−356.
(27) Li, L.; Zhong, Y. W.; Ma, C. Y.; Li, J.; Chen, C. K.; Zhang, A. J.; Tang, D. L.; Xie, S. Y.; Ma, Z. *Chem. Mater.* **2009**, *21* (20), 4977−4983.
(28) Shah, P. S.; Sigman, M. B.; Stowell, C. A.; Lim, K. T.; Johnston, K. P.; Korgel, B. A. *Adv. Mater.* **2003**, *15* (12), 971−974.
(29) Stenzel, M. H.; Davis, T. P.; Fane, A. G. *J. Mater. Chem.* **2003**, *13* (9), 2090−2097.
(30) Kadla, J. F.; Asfour, F. H.; Bar-Nir, B. *Biomacromolecules* **2007**, *8* (1), 161−165.
(31) Wong, K.; Hernández-Guerrero, M.; Granville, A.; Davis, T.; Barner-Kowollik, C.; Stenzel, M. *J. Porous Mater.* **2006**, *13* (3), 213−223.
(32) Bock, V. D.; Hiemstra, H.; van Maarseveen, J. H. *Eur. J. Org. Chem.* **2006**, *2006* (1), 51−68.
(33) Fokin, V. V.; Rostovtsev, V. V.; Green, L. G.; Sharpless, K. B. *Angew. Chem., Int. Ed.* **2002**, *41* (14), 2596−2599.
(34) Kolb, H. C.; Sharpless, K. B. *Drug Discovery Today* **2003**, *8* (24), 1128−1137.
(35) Bryan, M. C.; Fazio, F.; Lee, H. K.; Huang, C. Y.; Chang, A.; Best, M. D.; Calarese, D. A.; Blixt, C.; Paulson, J. C.; Burton, D.; Wilson, I. A.; Wong, C. H. *J. Am. Chem. Soc.* **2004**, *126* (28), 8640−8641.
(36) Wang, Q.; Chan, T. R.; Hilgraf, R.; Fokin, V. V.; Sharpless, K. B.; Finn, M. G. *J. Am. Chem. Soc.* **2003**, *125* (11), 3192−3193.
(37) Link, A. J.; Tirrell, D. A. *J. Am. Chem. Soc.* **2003**, *125* (37), 11164−11165.
(38) Nystrom, D.; Malmstrom, E.; Hult, A.; Blakey, I.; Boyer, C.; Davis, T. P.; Whittaker, M. R. *Langmuir* **2010**, *26* (15), 12748−12754.
(39) Koschella, A.; Heinze, T.; Klemm, D. *Macromol. Biosci.* **2001**, *1* (1), 49−54.
(40) Bar-Nir, B. B.-A.; Kadla, J. F. *Carbohydr. Polym.* **2009**, *76* (1), 60−67.
(41) Lin, P.-C.; Ueng, S.-H.; Yu, S.-C.; Jan, M.-D.; Adak, A. K.; Yu, C.-C.; Lin, C.-C. *Org. Lett.* **2007**, *9* (11), 2131−2134.